




RESEARCH ARTICLE | JUNE 23 2022

Resonant torque differential magnetometry with high frequency quartz oscillators

Guoxin Zheng ; Dechen Zhang; Kuan-Wen Chen; John Singleton; Lu Li  

 Check for updates

Rev. Sci. Instrum. 93, 063907 (2022)

<https://doi.org/10.1063/5.0084231>

 CHORUS



View Online



Export Citation

CrossMark

AIP Advances

Why Publish With Us?



25 DAYS
average time
to 1st decision



740+ DOWNLOADS
average per article



INCLUSIVE
scope

[Learn More](#)




Resonant torque differential magnetometry with high frequency quartz oscillators

Cite as: *Rev. Sci. Instrum.* **93**, 063907 (2022); doi: [10.1063/5.0084231](https://doi.org/10.1063/5.0084231)

Submitted: 7 January 2022 • Accepted: 1 June 2022 •

Published Online: 23 June 2022



View Online



Export Citation



CrossMark

Guoxin Zheng,¹  Dechen Zhang,¹ Kuan-Wen Chen,¹ John Singleton,² and Lu Li^{1,a)} 

AFFILIATIONS

¹ Department of Physics, University of Michigan, Ann Arbor, Michigan 48109, USA

² National High Magnetic Field Laboratory, MS E536, Los Alamos National Laboratory, Los Alamos, New Mexico 87545, USA

^{a)} Author to whom correspondence should be addressed: luli@umich.edu

ABSTRACT

Sensitive magnetometry has been a powerful probe for investigating quantum materials. Extreme conditions, such as sub-kelvin cryogenic temperatures and ultrahigh magnetic fields, demand further durability for sensitive magnetometry. However, significant mechanical vibrations and rapid magnetic field changes give enormous challenges to conventional magnetometry. This article presents a possible solution to this problem by developing a new magnetometry technique using high-frequency quartz oscillators. The technique takes advantage of the symmetry and geometry of mechanical vibration configurations of standard commercially available MHz quartz oscillators, and the setup keeps the high quality factor resonance with the sample mounted on the oscillator. We further demonstrate the sensitivity of the technique using bismuth single crystals and a $\text{Fe}_{0.25}\text{TaS}_2$ ferromagnetic material. Quantum oscillations are observed in the magnetometry response below 1 T, and the detected oscillation frequency is shown to come from the electron pockets of the bismuth.

Published under an exclusive license by AIP Publishing. <https://doi.org/10.1063/5.0084231>

I. INTRODUCTION

Sensitive magnetometry is a powerful probe for the research and development of solid state quantum materials and devices. Take the example of correlated quantum materials in which strong electron interactions often lead to exotic physical phenomena. Resolving the magnetic ground state as well as quantum oscillations requires sensitive magnetometry in intense magnetic fields as high as 30–80 T.^{1,2} There are several magnetometry techniques already developed for the operation in pulsed fields, including micromechanical trampoline magnetometers³ and cantilever magnetometry.⁴ However, the trampoline magnetometer is better suited to small samples ($\sim 1 \mu\text{g}$). The cantilever magnetometry is limited to a frequency response below 5 kHz and thus only suitable for long pulse magnets (~ 0.1 –1 s duration). Therefore, the rapid progress in quantum materials calls for new sensitive magnetometry that can particularly adapt to short intense pulsed magnetic fields.

To shed light on the electronic and magnetic structures in quantum materials, we recently developed a resonant torque differential magnetometry using the cantilever differential torque resonance mode of a quartz tuning fork⁵ (the “qPlus” mode^{6,7}), which

resonates at ~ 30 kHz and is typically not fast enough to respond to the quantum oscillation (QO) features in the intense fields of pulsed magnets. The old-generation cantilever-based magnetometry in intense DC magnets is always coupled with mechanical vibrations. High-quality resonant magnetometry decouples nicely from low frequency mechanical noise. Indeed, this early work using quartz tuning forks established a powerful torque differential magnetometry⁵ that works well in DC magnets. However, a technical challenge still exists due to a relatively low 32 kHz resonance frequency, limiting the application of this resonant magnetometry in other extreme conditions, particularly in pulsed magnets in which the magnetic field changes by 100 T within a few milliseconds. More importantly, the quartz tuning fork magnetometry setup loses its resonance once immersed in liquid ³He or liquid ⁴He. Therefore, resonant magnetometry needs to be more stable at higher frequencies and should maintain its resonance in a cryogenic liquid environment.

The resonance of quartz crystals has been core to the stable frequency references for computers chips.⁸ The typical symmetric design helps the oscillator run in vibration modes that are not easily affected by the environmental temperatures. Nevertheless,

this advantage raises a crucial challenge to the idea of magnetometry application—regardless of its size and magnetic properties, any solid state sample attached to a quartz crystal breaks the symmetry.

This article demonstrates a new technique for quartz oscillator torque differential magnetometry that achieves a large quality factor (Q -factor). We test the quartz oscillator with different sample mounting positions on the rotator probe of a Janis variable temperature insert (VTI) system, which provides a low temperature environment. We further demonstrate the high sensitivity of our quartz oscillator torque differential magnetometry by measuring the de Haas–van Alphen (dHvA) effect in a bismuth single crystal. Quantum oscillations are resolved under the magnetic field using different detection circuits, and the observed frequency and effective mass are consistent with the Fermi surface obtained in the previous results.⁹ We also demonstrate the feasibility of exploiting our oscillator magnetometry in a fast, pulsed magnetic field by measuring the dHvA effect in bismuth samples. The observed quantum oscillations are highly consistent with our DC field, VTI measurement results. In addition, we determined the order of magnitude of magnetization sensitivity of MHz oscillator magnetometry by measuring the hysteresis loops in the $\text{Fe}_{0.25}\text{TaS}_2$ ferromagnetic material.

II. EXPERIMENTAL SETUP

The first important step is taking the quartz crystal out of the package and leads. The packaging case and electrical leads are magnetic, which will strongly affect the performance of magnetic sensing. The quartz crystal we used has the cylindrical type package case, which is much easier to remove than the rectangular case. One way to take the quartz crystal out of the package is to put the case on the table and then use a steel file to roll it back and forth modestly until the inside quartz crystal with leads detaches from the outer case. Next is to fix the electrical leads with a bench vise and melt the bottom solder joints with a torch. While the joints are melting, the quartz crystal can be taken out quickly using a tweezer. Pictures of the package quartz oscillator (Model No. AB308-4.000 MHz of Vendor Abracon LLC) and the bare oscillator are shown in Figs. 1(a) and 1(b).

We chose single crystals of elemental bismuth (Bi) for the testing samples because they established sharp Landau-level quantization patterns in our early low-frequency differential magnetometry⁵ as well as the rich physics of Dirac electrons in magnetic fields.⁹ As shown in Fig. 1(c), we tested sample mountings in two different methods: an asymmetric method (ASYM) and a symmetric method (SYM). Because the edge part of a quartz oscillator has nearly no influence on the resonance frequency,¹¹ one edge of the quartz oscillator is anchored on the “L” shape sapphire substrate by thermal epoxy (Model H74F of Vendor EPOXY). The gold wires are firmly glued near the edge of the oscillator using a silver epoxy (Model H20E) to ensure they have the minimum influence on the Q -factor. This setup compares the response of the thickness-shear mode of quartz.¹⁰ The mathematical physical analysis of the thickness-shear mode can be found in Refs. 11 and 12. The Bi crystals were cut to $0.5 \times 0.43 \times 0.2 \text{ mm}^3$ and glued to the oscillators permanently with the thermal epoxy. In the following, we will compare the resonance frequency response under the magnetic fields of these two

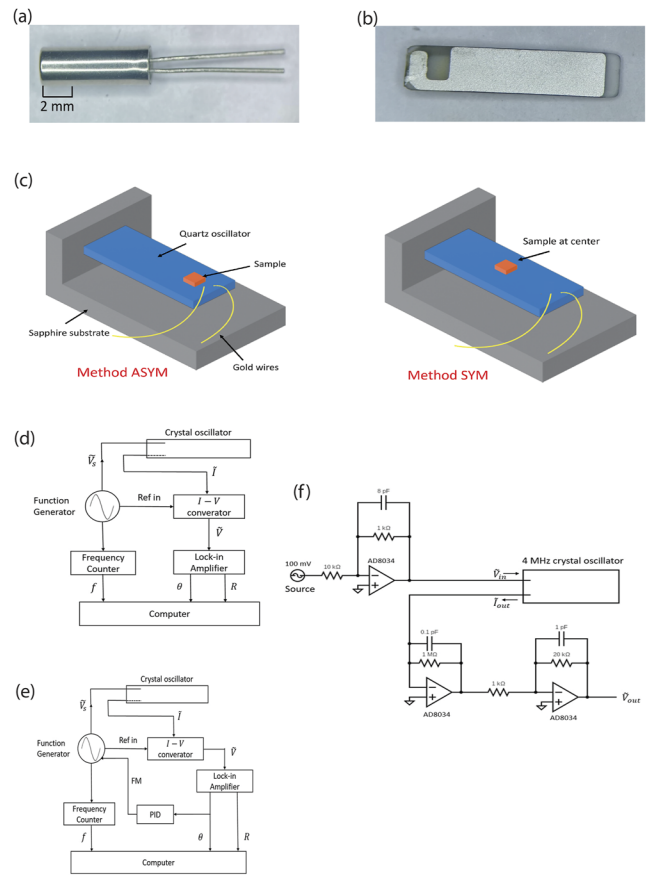


FIG. 1. Experimental setup: (a) Pictures of quartz oscillator Model No. AB308-4.000 MHz of Vendor Abracon LLC as purchased. (b) Picture of the oscillator after the metallic case and electrical leads are removed. (c) Schemes for mounting method ASYM and method SYM. The quartz oscillators are anchored on the sapphire substrate. (d) Diagram for the direct mode detection circuit. (e) Diagram for the PID mode feedback detection circuit. (f) Design diagram of the current–voltage converter.

methods. Further characterization of the same resonance magnetometer with Bi was tested using the 65 T pulsed magnet using the Pulsed Magnetic Field Facility in Los Alamos National Laboratory (LANL). A DC response of a ferromagnet $\text{Fe}_{0.25}\text{TaS}_2$ crystal was measured with the same ASYM method to estimate the sensitivity of this magnetometry technique.

Following the schemes of Ref. 5, the quartz oscillators are driven with a sinusoidal voltage of a function generator. The generated currents are measured by a lock-in amplifier Stanford Research SR 844 either using the current-input-mode of the lock-in amplifier or through a home-built I – V converter. The design of the I – V converter is shown in Fig. 1(f). Once the resonance is detected, we apply a magnetic field and detect the shift of the resonance using two available detection modes: the direct mode [Fig. 1(d)] and the proportional integral differential (PID) mode [Fig. 1(e)]. The lock-in output signals are directly recorded in the direct mode as the amplitude and the phase. In the PID mode, a phase-locked loop

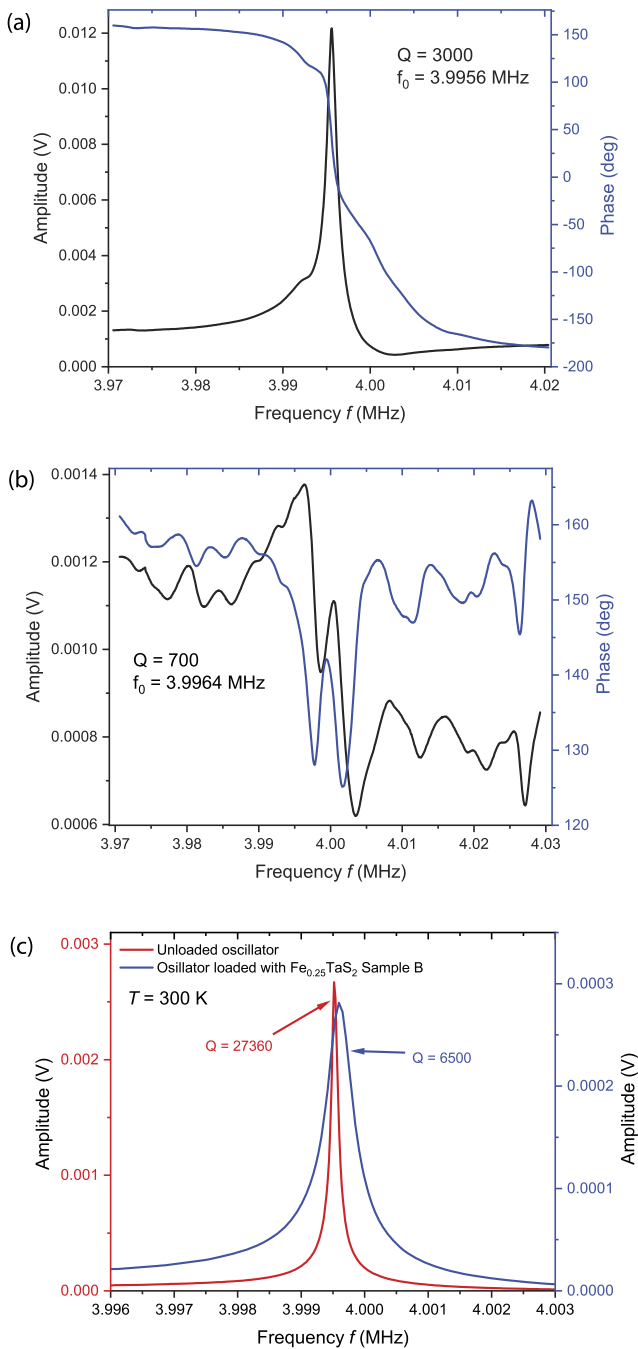


FIG. 2. Resonance of quartz oscillators mounted with bismuth (a) and (b) and $\text{Fe}_{0.25}\text{TaS}_2$ (c) single crystals. (a) When a bismuth sample is mounted to a quartz oscillator using the asymmetric (ASYM) method, a sharp resonance appears when the driving frequency is tuned close to 4 MHz at 3 K. (b) In contrast, the quartz oscillator can barely resonate when a sample is mounted in the SYM way. (c) Comparison between the resonance peaks of an unloaded oscillator (red curve), which has a Q -factor 27 360, and the same oscillator loaded with $\text{Fe}_{0.25}\text{TaS}_2$ sample B (blue curve) using the ASYM method leads to a Q -factor 6500. The measurement temperature is 300 K.

feedback circuit is built using a PID controller to keep the oscillation at the resonance.⁵ As established in Ref. 5, both the phase in the direct mode and the frequency change in the PID mode are proportional to the differential torque $d\tau/d\theta$, with the magnetic torque $\tau = \mathbf{m} \times \mathbf{B}$, and the magnetic field tilt angle θ between the sample magnetic moment \mathbf{m} and magnetic field \mathbf{B} .

III. RESULTS

Figures 2(a) and 2(b) show the output signals of a quartz oscillator with a Bi crystal mounted in the ASYM method [panel (a)] and the SYM method [panel (b)]. The test was carried out at $T = 3$ K. The ASYM method shows a clear resonance with a Q -factor *sim* 3000, much better than the resonance in the device mounted in the SYM method. Therefore, in the following tests, we will focus on the measurements only on oscillator devices mounted in the ASYM method. Figure 2(c) shows the comparison between the resonance peaks of an unloaded oscillator (red curve) and the same oscillator loaded with $\text{Fe}_{0.25}\text{TaS}_2$ sample B (blue curve) measured at room temperature using the ASYM method. After loading the sample, the Q -factor dropped from 27 360 to 6500, and the resonance frequency decreased by 80 Hz, which is expected because the loaded sample will destroy the original symmetric thickness-shear mode and shift to a new resonance frequency.

We applied a magnetic B field to the device with the B -field about 15° away from the long axis of the quantum oscillator and the Bi crystal mounted in the ASYM method. Figure 3 shows the response using both the direct mode circuit and the PID mode circuit. The phase shift in the direct mode closely tracks the frequency change in the PID mode, which directly detects the differential torque signal. The results demonstrate the oscillatory patterns are in the magnetic signals of semimetal Bi, which results from the Landau level quantizations of Dirac electron and hole Fermi surfaces.⁹

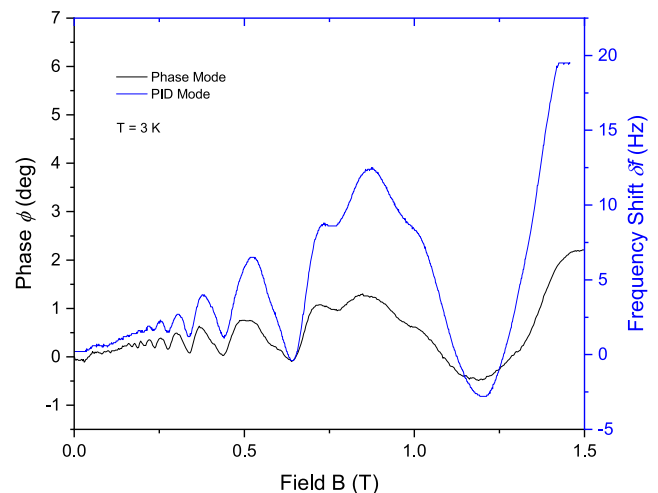


FIG. 3. Result of the differential magnetometry using the MHz quartz oscillators and a Bi crystal mounted in the ASYM method. (a) Both the direct mode and the PID mode detect the large oscillatory magnetic signals of Bi due to the Landau level quantization under the B -field.

To confirm the Landau level quantization of the oscillatory pattern, the oscillatory parts of phase ϕ were taken by subtracting the polynomial backgrounds. As shown in Fig. 4(a), the oscillatory patterns $\Delta\phi$ are clearly periodic in $1/B$ for all tested temperatures T . We determine the oscillation frequency with the Fast Fourier transform of the $\Delta\phi$, which is shown in Fig. 4(b), and the dominating oscillation frequency is about 1.5 T, which is consistent with the Fermi surface orbital size in the B -field orientation.⁹ Furthermore, the peak amplitude of this dominating frequency is tracked with T in Fig. 4(c), and the temperature dependence is consistent with the Lifshitz–Kosevich (LK) formula¹³

$$\rho_{xx}^{osc}(T) \propto \frac{\frac{2\pi^2 k_B m^* T}{e\hbar\mu_0 H}}{\sinh\left(\frac{2\pi^2 k_B m^* T}{e\hbar\mu_0 H}\right)}, \quad (1)$$

where m^* is the cyclotron mass for motion in the plane perpendicular to the applied H . The comparison shows $m = 0.011m_e$, with m_e being the bare electron mass, which is consistent with the light

effective mass of electron orbit in this field orientation. Finally, the orbital size is consistent with the Bi electronic structure. Figure 4(d) shows the angular dependence of the dominating oscillation period as the magnetic field direction is changed in the crystalline plane of the binary axis and the trigonal axis. The angular dependence demonstrates a roughly symmetric pattern and the oscillation period is consistent with that from the expectation of electron Fermi surface pockets.

After demonstrating the high sensitivity of our oscillator magnetometry in the DC magnet, we measure the response of the same MHz oscillator magnetometry in pulsed magnets in LANL. Figure 5 shows the quantum oscillations of the Bi sample measured by the MHz oscillator magnetometry using direct mode, compared with the results measured in the VTI system. The subtle QO frequency difference should come from the setup alignment. The same quantum oscillation patterns prove the usability of oscillator magnetometry in the fast pulsed magnetic field, and the response time of our oscillator magnetometry is short enough to catch the magnetic features. A typical profile of a field pulse can be seen in Fig. 6(a). The

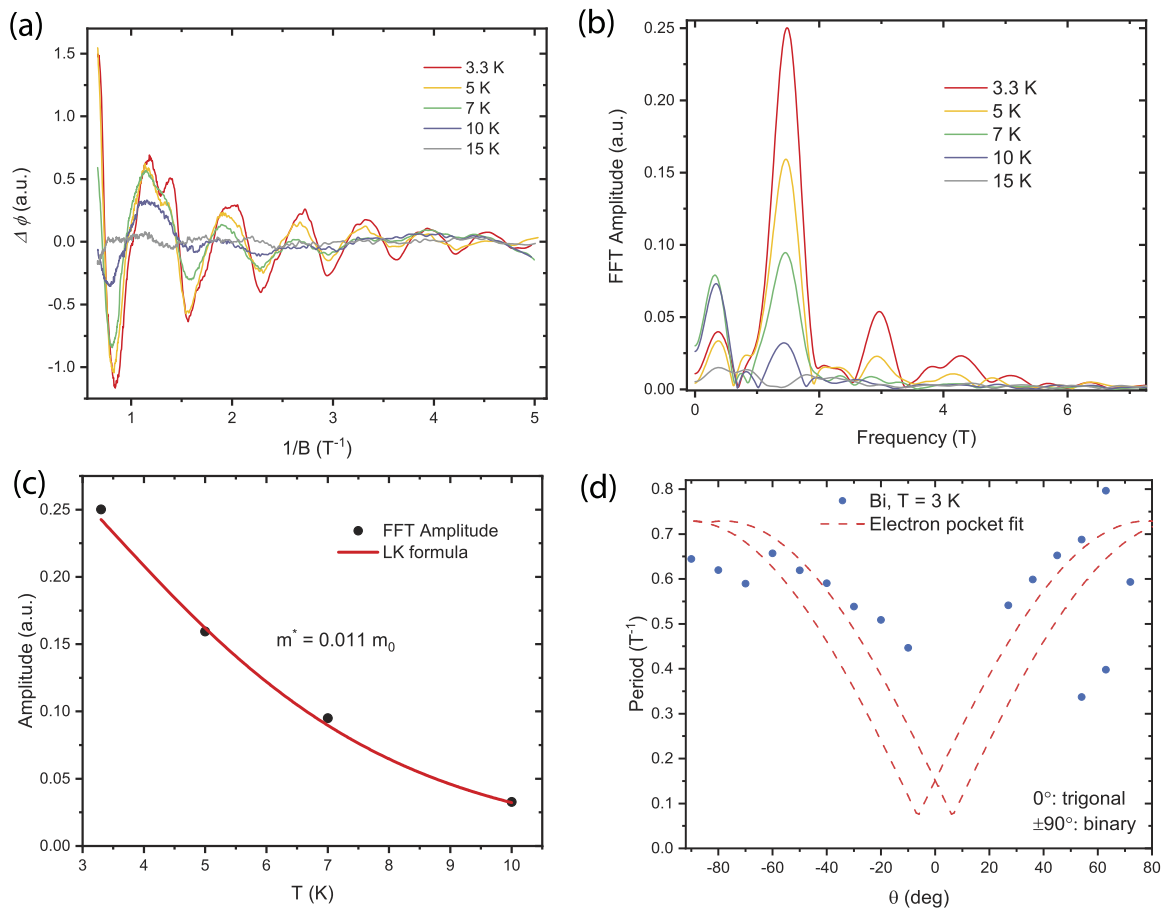


FIG. 4. Landau level quantization analysis for the quantum oscillation signals detected by the resonant torque differential magnetometry. (a) After subtracting the polynomial background, the oscillation pattern is periodic in $1/B$, taken at selected T . (b) A fast Fourier transformation analysis shows the dominating oscillation frequency. (c) The oscillation amplitude of the dominating frequency is plotted as a function of T , which is consistent with the LK formula. (d) The angular dependence of the oscillation period.

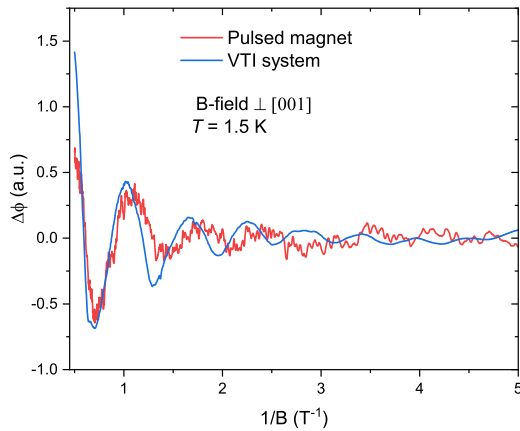


FIG. 5. Result of the quantum oscillations measured by the MHz oscillator magnetometry with a Bi sample mounted in the pulsed magnetic field (red curve), compared with the quantum oscillations of the same Bi sample measured in the VTI magnet (blue curve). The magnetic field is approximately perpendicular to the [001] direction. Both curves were measured by direct mode, and the phase changes $\Delta\phi$ are plotted after background subtraction with the inverse of the magnetic field. The result in the pulsed magnet was taken when the field was down from the maximum to zero.

magnetic field pulse total duration time is less than 80 ms, with a rise time of 8 ms, and Fig. 6(b) shows the response of quartz oscillator with Bi sample at 1.5 K. The field was down from the maximum to zero when the data were taken. From Fig. 5, we notice that one problem with using the MHz oscillator magnetometry in the pulsed

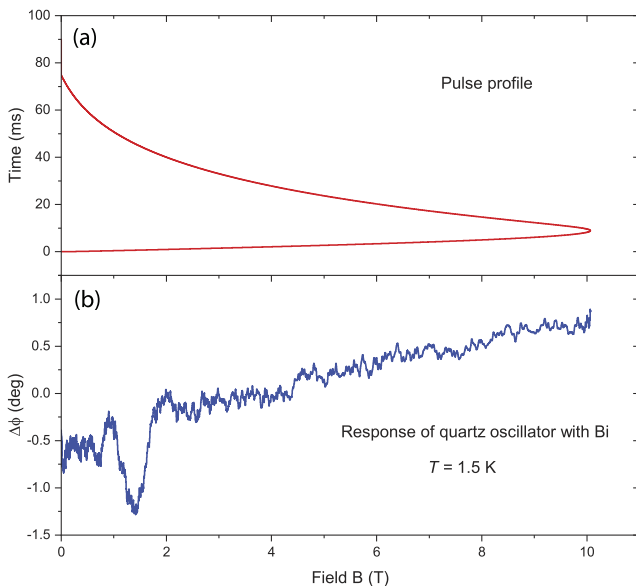


FIG. 6. (a) Profile of magnetic field pulse duration in a short pulse magnet in LANL. (b) The change of phase of quartz oscillator with Bi sample mounted measured by direct mode at 1.5 K, measured in the down-sweep of the pulsed magnet.

field is the noise level. The blue curve taken in the DC field has a much lower noise level than the red curve taken in the pulsed field in Fig. 5. While the red and blue curves measured the same magnetization signal, we can make a quick sensitivity estimation on the DC field and pulsed field. The phase resolution of the blue curve in Fig. 5 is around 0.02° , while the resolution of the red curve is about 0.1° . Therefore, the sensitivity of MHz oscillator magnetometry in the pulsed field is five times worse than in the DC field. One important reason for the difference is the vibration-induced noise in the pulsed field is much larger than in the DC field. Another reason could be the difference in data acquisition instruments. In the DC field, the data are acquired from the SR 844 lock-in amplifier, while in the pulsed field, the data are obtained by the National Instruments Data Acquisition card, which has a higher noise level and does not have a pre-filter. Thus, future development is needed to reduce the vibration noise and design appropriate filters. Moreover, this current quartz oscillator setup is too long to fit into the narrow rotator probe in the LANL pulsed field magnets due to the small magnet bore sizes. For future experiments, we will search for smaller quartz oscillators that can fit into these rotator probes used in the LANL pulsed field magnets.

Sensitivity and response time are two critical attributes of our quartz magnetometer in the pulsed field. The 4 MHz resonance frequency can provide a fast enough response time to catch the QOs in bismuth without lag in the short pulsed field, as shown in Fig. 5. Next, to estimate the sensitivity and calibrate the order of magnitude of the magnetic moment measured by the MHz quartz oscillator, we measure the hysteresis loop of a well-studied ferromagnetic material $\text{Fe}_{0.25}\text{TaS}_2$. The $\text{Fe}_{0.25}\text{TaS}_2$ samples were grown by the chemical vapor deposition method.¹⁵ The magnetization of this material is extremely anisotropic, with the magnetic moments aligned parallel to the c crystallographic direction.^{15,16}

Magnetization is taken with the Quantum Design Physical Property Measurement System (PPMS) using the vibrating-sample magnetometer (VSM) option at 2 K. The $\text{Fe}_{0.25}\text{TaS}_2$ sample A measured in PPMS has a dimension of $1.25 \times 0.625 \times 0.025 \text{ mm}^3$. A sharp hysteresis loop is observed when $H \parallel c$, as shown in Fig. 7(a). The magnetization saturates at 5.3 T, and the saturation magnetic moment is around $m_{sA} \sim 2.6 \times 10^{-3} \text{ emu}$. The torque differential of $\text{Fe}_{0.25}\text{TaS}_2$ sample B is measured by the PID mode of MHz quartz oscillator in Janis VTI system at 2 K, as shown in Fig. 7(b). The dimension of sample B is $0.6 \times 0.26 \times 0.013 \text{ mm}^3$. The angle θ between the field and c axis is 4.4° . The torque differential response and transition field are consistent with the magnetization in Fig. 7(a). The hump around -3.5 T can be attributed to the environment noise. The frequency shift Δf corresponding to the magnetic transition at 5.3 T in the torque differential response is about 16.5 Hz. Then, we can estimate the saturation magnetic moment of sample B by comparing the sample size, which is $m_{sB} \sim 2.7 \times 10^{-4} \text{ emu}$. We should notice this is the saturation magnetic moment when field along c axis. We know

$$\Delta f \propto \frac{\partial \tau}{\partial \theta} \approx mB \cos \theta. \quad (2)$$

When $\theta = 4.4^\circ$, $\Delta f(\theta = 4.4^\circ) = 16.5 \text{ Hz}$, so $\Delta f(\theta = 0^\circ) = \Delta f(\theta = 4.4^\circ) / \cos \theta = 16.55 \text{ Hz}$. Furthermore, the sensitivity of magnetic moment can be estimated as

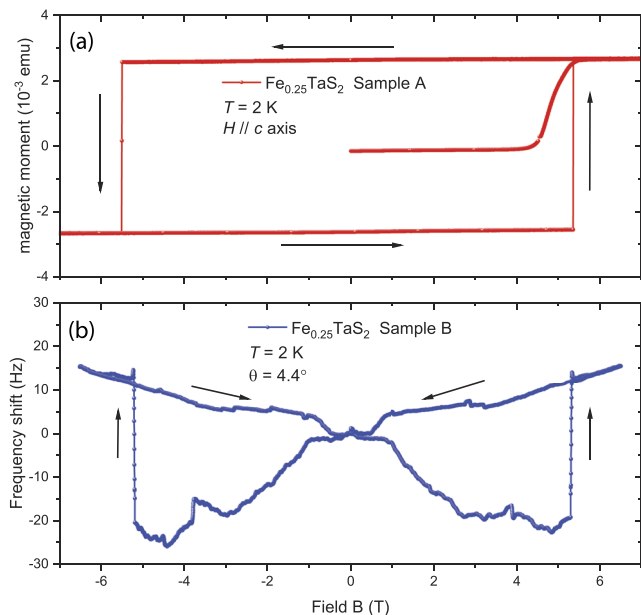


FIG. 7. Hysteresis loop in $\text{Fe}_{0.25}\text{TaS}_2$. (a) Magnetic moment curves for $H \parallel c$ measured by VSM in sample A at 2 K. (b) Frequency shift vs magnetic field measured by a MHz quartz oscillator PID mode in sample B at 2 K. θ is the angle between field and c axis.

$$\delta m = \frac{\delta f}{\Delta f(\theta = 0^\circ)} \times \Delta m_{sB}. \quad (3)$$

Here, δf is the uncertainty of frequency measurement, which comes from the output of PID. The uncertainty for the PID output is about 3×10^{-3} V, which corresponds to $\delta f = 0.03$ Hz. Finally, the sensitivity of magnetic moment is estimated at $\delta m \sim 4.9 \times 10^{-7}$ emu at 5 T, which is comparable to the best claimed sensitivity of the latest Magnetic Property Measurement System (MPMS) ($\sim 8 \times 10^{-8}$ emu at 5 T) by Quantum Design.

IV. DISCUSSION

Our results based on semimetal Bi demonstrated the power of the ASYM mounting method for resonant magnetometry for solid state quantum materials. As mentioned in the Introduction, the method took advantage of the thickness-shearing mode and kept the high- Q resonance even with sizable target samples. In the 1990s, the scanning microscopy community realized using the q-plus mode¹⁴ to the quartz tuning forks to isolate only one mode for the detection of the magnetic force gradient for the atomic force microscopy (AFM) and magnetic force microscopy (MFM). After two decades, almost all the high-end commercial AFM and MFM instruments are based on this q-plus mode tuning fork application. We believe that our new ASYM mode is a similar resolution step. Therefore, we may envision magnetometry as what we demonstrate in the results. We propose using the ASYM mode to mount the AFM tip or MFM tip to the high-frequency quartz oscillator for advanced microscopy. The higher resonance frequency is more likely decoupled from mechanical vibrations. We note further that the ASYM

setup is robust: the resonance keeps the high Q -factor in a vacuum and cryogenic gas environments and cryogenic liquids, such as liquid ^4He and liquid ^3He . These are just a few technical advantages of using the ASYM mounting method and the quartz oscillators for experiments in solid state materials.

In summary, we developed the asymmetric (ASYM) mode mounting method in quartz oscillators for magnetometry for solid state materials. The test with Bi single crystals revealed clear quantum oscillation patterns due to the Landau Level quantizations of the electronic pockets both in DC and pulsed magnetic field. We estimated the sensitivity of magnetic moment measured by the MHz oscillator magnetometry by measuring the hysteresis loop of $\text{Fe}_{0.25}\text{TaS}_2$ ferromagnetic material. Furthermore, the high- Q resonance in the MHz resonance frequencies indicates the great potential for the application in magnetometry and even for scanning microscopies.

ACKNOWLEDGMENTS

This work was mainly supported by the Department of Energy under Award No. DE-SC0020184. We thank Dr. John Singleton of LANL for the test run of our quartz oscillator in the pulsed magnetic fields and Professor Xianhui Chen of the University of Science and Technology of China for the $\text{Fe}_{0.25}\text{TaS}_2$ crystals. A portion of this work was performed at the National High Magnetic Field Laboratory (NHMFL), which is supported by National Science Foundation Cooperative Agreement No. DMR-1644779 and the Department of Energy (DOE).

AUTHOR DECLARATIONS

Conflict of Interest

The authors have no conflicts to disclose.

Author Contributions

Guoxin Zheng: Conceptualization (lead); Formal analysis (lead); Methodology (lead); Writing – original draft (equal). **Dechen Zhang:** Data curation (supporting). **Kuan-Wen Chen:** Data curation (supporting). **John Singleton:** Methodology (supporting). **Lu Li:** Conceptualization (lead); Funding acquisition (lead); Supervision (lead); Writing – original draft (equal); Writing – review & editing (equal)

DATA AVAILABILITY

The data that support the plots within this paper and other findings of this study are available from the corresponding author upon reasonable request.

REFERENCES

- Z. Xiang, L. Chen, K.-W. Chen, C. Tinsman, Y. Sato, T. Asaba, H. Lu, Y. Kasahara, M. Jaime, F. Balakirev, F. Iga, Y. Matsuda, J. Singleton, and L. Li, *Nat. Phys.* **17**, 788 (2021).
- L. Li, K. Sun, C. Kurdak, and J. W. Allen, *Nat. Rev. Phys.* **2**, 512 (2020).
- V. Aksyuk, F. F. Balakirev, G. S. Boebinger, P. L. Gammel, R. C. Haddon, and D. J. Bishop, *Science* **280**, 720 (1998).

- ⁴M. J. Naughton, J. P. Ulmet, A. Narjis, S. Askenazy, M. V. Chaparala, and A. P. Hope, *Rev. Sci. Instrum.* **68**, 4061 (1997).
- ⁵L. Chen, F. Yu, Z. Xiang, T. Asaba, C. Tinsman, B. Lawson, P. M. Sass, W. Wu, B. Kang, X. Chen, and L. Li, *Phys. Rev. Appl.* **9**, 024005 (2018).
- ⁶F. J. Giessibl, *Rev. Sci. Instrum.* **90**, 011101 (2019).
- ⁷F. J. Giessibl, *Appl. Phys. Lett.* **73**, 3956 (1998).
- ⁸E. A. Vittoz, M. G. R. Degrauwe, and S. Bitz, *IEEE J. Solid-State Circuits* **23**, 774 (1988).
- ⁹L. Li, J. G. Checkelsky, Y. S. Hor, C. Uher, A. F. Hebard, R. J. Cava, and N. P. Ong, *Science* **321**, 547 (2008).
- ¹⁰J. R. Vig, NASA STI/RECON Technical Report No. 9519519, 1994.
- ¹¹Y.-K. Yong and J. T. Stewart, *IEEE Trans. Ultrason., Ferroelectr. Freq. Control* **38**(1), 67 (1991).
- ¹²J. Wang, W. Zhang, D. Huang, T. Ma, J. Du, and L. Yi, paper presented at the 2015 Joint Conference of the IEEE International Frequency Control Symposium and the European Frequency and Time Forum, 2015.
- ¹³D. Shoenberg, *Magnetic Oscillations in Metals* (Cambridge University Press, 2009).
- ¹⁴P. Günther, U. C. Fischer, and K. Dransfeld, *Appl. Phys. B: Photophys. Laser Chem.* **48**, 89 (1989).
- ¹⁵G. Wu, B. L. Kang, Y. L. Li, T. Wu, N. Z. Wang, X. G. Luo, Z. Sun, L. J. Zou, and X. H. Chen, "Large magnetic anisotropy in FexTaS₂ single crystals," [arXiv:1705.03139](https://arxiv.org/abs/1705.03139) (2017).
- ¹⁶E. Morosan, H. W. Zandbergen, L. Li, M. Lee, J. G. Checkelsky, M. Heinrich, T. Siegrist, N. P. Ong, and R. J. Cava, *Phys. Rev. B* **75**, 104401 (2007).